Investigation of Infiltration Loss in North Central Texas by Retrieving Initial Abstraction and Constant Loss from Observed Rainfall and Runoff Events

Jiaqi Zhang[1]; Shang Gao[2]; and Zheng Fang, M.ASCE[3]

Abstract: Accurate modeling of infiltration losses is vital for runoff estimation and thus the development of flood design/protection criteria and water management schemes, etc. In design flood practices, the initial abstraction and constant loss (IACL) method has been widely applied due to its simplicity. However, due to a lack of physical equivalent properties, the IACL method is often subject to issues in parametrization and has large dependency on calibration efforts for storm events. Despite the wide range/variability of IACL values, a single set of IA and CL values is normally adopted for specific flood frequency, which may introduce uncertainty and bias in resulting peak streamflow. In this study, we identified a total of 2,036 rainfall-runoff events for 18 watersheds in North Central Texas to estimate the total losses with their IA and CL components based on time-series of mean areal precipitation (MAP) and streamflow data. Threshold behavior is found for all studied subbasins between the summation of gross rainfall and antecedent soil moisture versus runoff depth: below the threshold, runoff depth is minimal; whereas above it, runoff is largely linearly correlated with the summation of rainfall and antecedent soil moisture. This finding provides a convenient way to estimate/predict total loss or runoff depth given MAP and antecedent soil moisture. In addition, this study shows that the IA and CL values can be approximated by the gamma and Weibull distributions, respectively. The fitted distributions of IA and CL values can be applied in a Monte Carlo simulation framework to stochastically simulate numerous rainfall-runoff events for a flood frequency analysis. **DOI: 10.1061/JHYEFF.HEENG-5883.**

Author keywords: Infiltration losses; Antecedent soil moisture (ASM); Rainfall and runoff; Threshold behavior; Initial abstraction (IA); Constant loss (CL); Distribution; Design event; Flood frequency.

Introduction

As a fundamental component in hydrologic cycle, infiltration losses have drawn much research attention throughout the history of hydrology. Accurate modeling of infiltration losses is important for runoff estimation and can facilitate the development of flood design/protection criteria and water management schemes, etc. Infiltration models can be generally classified as three types (Mishra et al. 2003): physically based (or theoretical/mechanistic), semiempirical, and empirical/conceptual models. Physically based models refer to an approach that is close to physical theory and has an analytical solution, such as Green and Ampt (1911), Richards (1931), Phillip (1957, 1969), Mein and Larson (1971, 1973), and Smith (1972), etc. Semiempirical models are based on simplified continuity equations with certain hypotheses (e.g., Horton 1938; Holtan 1961; Overton 1964; Burnash et al. 1973; Singh and Yu 1990). Empirical/conceptual models are derived from experimental observations and represent the overall infiltration process (Singh and Yu 1990). Examples of such models are SCS-Curve (Mockus and Hjelmfelt 1972), Collis-George (1977), initial abstraction and constant loss (IACL) models (USACE 1992), etc.

Among numerous infiltration loss models, the IACL method is applied in many engineering practices (USACE 1992; Heneker 2002; Rahman et al. 2002a; Hill et al. 2016). The concept of IACL is that any watershed is assumed to store an absolute depth of rainfall at the beginning of a storm as initial abstraction (IA) and then reduce the rainfall at a constant loss (CL) rate (Asquith and Roussel 2007). Therefore, in IACL method, two different losses are used: (1) the initial loss/initial abstraction (IA) in mm which must be satisfied before any runoff occurs; and (2) a constant loss (CL) in mm-per-hour which continues after the initial loss has been satisfied. If a storm event generates rainfall less than IA, no runoff will be produced. For any runoff-generating storm events, the total loss consists of two loss components resulted from IA and CL, respectively.

Due to its simplicity and ability to approximate overall catchment runoff behavior, IACL is usually adopted to estimate infiltration losses for design frequency storms (USACE 1992; Hill et al. 2016). For ungauged areas, estimating losses to convert the design rainfall into design peak streamflow is known as the design event approach in flood frequency studies (USACE 1992; Rahman et al. 2002a; USACE 2013). The design event approach, or rainfall-based design flood estimation method, assumes that the frequency of the input rainfall depth can be preserved in the final flood output (streamflow) by selecting design values of other model parameters (e.g., infiltration loss, unit hydrograph, and routing parameters) in the rainfall-runoff modeling (Charalambous et al. 2013). At present, there is no specific guidelines on how to select the proper IACL values for design and the choice highly depends on certain assumptions and individual designers.

[1]Postdoctoral Research Associate, School of Civil Engineering and Environmental Sciences, Univ. of Oklahoma, Norman, OK 73019. ORCID: https://orcid.org/0000-0003-1071-6742. Email: jiaqi.zhang@ou.edu

[2]Postdoctoral Research Associate, School of Civil Engineering and Environmental Sciences, Univ. of Oklahoma, Norman, OK 73019. Email: shang.gao@ou.edu

[3]Associate Professor, Dept. of Civil Engineering, Univ. of Texas at Arlington, Arlington, TX 76019 (corresponding author). ORCID: https://orcid.org/0000-0001-9871-8405. Email: nickfang@uta.edu

Note. This manuscript was submitted on July 25, 2022; approved on December 23, 2022; published online on March 2, 2023. Discussion period open until August 2, 2023; separate discussions must be submitted for individual papers. This paper is part of the ***Journal of Hydrologic Engineering***, © ASCE, ISSN 1084-0699.

The design IACL values recommended by US Army Corps of Engineers (USACE 1992) are based on the percentage of sandy and clayey soils. These standard values vary with storm frequencies and are documented in a reconnaissance report (USACE 1992) as shown in Table S1. This recommendation follows the design event approach, assuming the equality of return periods among rainfall, discharge, and IACL parameters. For instance, 100-yr rainfall can generate 100-year peak discharge with 100-year IACL values. Other than USACE, Texas Department of Transportation (TxDOT) and United States Geological Survey (USGS) have conducted computational and statistical analyses to parametrize IACL values for 92 applicable watersheds in Texas (Asquith and Roussel 2007; Thompson et al. 2008). They first utilized the observed rainfall and runoff to compute the storm-specific IACL values using a custom-built software. Then, for each watershed, multiple watershed characteristics were selected, e.g., main-channel length, curve numbers, etc. as predictors, and used to develop regression equations for estimating the optimal values of the mean IA and CL. In the USGS and TxDOT studies, it should be noted that estimation of IA and CL is for developing watershed-specific gamma unit hydrograph, which is rather different to the role in the design event approach.

Apart from the design events, IA and CL values associated with real storms are found to have a high degree of variability, indicating that watersheds may exhibit a wide range of antecedent soil moisture conditions (Rahman et al. 2002a), The parametrization of IA and CL values therefore largely depends on model calibrations from events to events, which may be subject to the simplicity and the lack of physical equivalent properties of IACL method. Despite this known variability, a single set of deterministic IA and CL values for specific design frequency is usually adopted in current design event approach. Because of the nonlinear behavior of the rainfall-runoff process, this may introduce a large degree of uncertainty and bias in the resulting design flood estimation (Rahman et al. 2002a; Loveridge et al. 2013). Furthermore, using a single set of IA and CL values ignores the probabilistic aspects of model variables, and the assumption of return period equality has been questioned and argued by many studies (e.g., Pilgrim and Cordery 1975; Kuczera et al. 2006; Viglione et al. 2009). Thus, considering probability aspects of IACL values without assuming an equality in return period could bring a substantial improvement of flood frequency analysis.

In contrast to the design event approach, which is to generate frequency flood from a single combination (Eagleson 1972; Beran 1973), the joint probability approach (JPA) recognizes that any design flood characteristics (e.g., peak streamflow) could result from different combinations of rainfall input and other flood producing factors (e.g., loss-related variables). For example, the same peak streamflow can be generated by a small rainfall event with wet antecedent soil moisture condition or a large rainfall with dry antecedent condition of the watershed (e.g., Rahman et al. 2002b; Viglione et al. 2009; Charalambous et al. 2013). Thus, from the joint probability approach, the distribution of the model outputs (e.g., streamflow and stage) can be directly estimated by simulating the likely combinations of inputs and parameter values, leading to better estimation of frequency design flows. Meanwhile, subjective criteria used to specify model inputs can be eliminated since the JPA treats model input and parameters as random variables (Rahman et al. 2002a). For frequency analyses using JPA, it is critical to accurately prescribe probability distributions of parameters (e.g., IA and CL) that can represent observed loss values.

In sum, whether it be the design event approach or the joint probability approach, it is imperative to ensure a close relevance of the IA and CL parameters to observed infiltration loss. Therefore, a rigorous, effective IACL retrieval scheme could help overcome the lack of physical equivalent properties to IA and CL. To this end, this study aims to facilitate regional IACL-related practices via an improved characterization of the parameters' probabilistic nature based on numerous retrieved values from rainfall and runoff observations. As a contribution to the field, this investigation will set a knowledge base and create incentives for building a probabilistic approach as an alternative to the currently employed deterministic IACL parametrization. This study is performed for the 18 headwater catchments located in North Central Texas via achieving the following objectives: (1) to build a rainfall-runoff event catalog using long-term observations of precipitation and streamflow and investigate the relationships among total rainfall depth, total loss and runoff volume; and (2) to retrieve IA and CL values based on the identified rainfall-runoff events and characterize their regional, probabilistic features by fitting to probability distributions.

The paper is organized as follows: The next section describes the methodology with the study area, data utilized, and event selection; the following section summarizes the results and conducts discussions; the final section provides the conclusions and suggestions for future work from this study.

Methodology

Study Area

The study area is in the Upper Trinity River Basin (UTRB), where undeveloped areas are located at headwaters while urban areas (the Greater Dallas-Fort Worth Metroplex) reside at mid- and downstream of the basin [Fig. 1(a)]. Since a large portion of the area within UTRB is pervious, it is challenging to account for infiltration loss in the hydrologic processes. Moreover, sitting in a region of temperate mean climatological conditions (USACE 2013), UTRB experiences occasional extremes of temperature and rainfall with relatively short durations. The complexity of the infiltration process combining with the climate variability brings challenges to engineering practices, especially in flood frequency analysis and flood forecasting. Fig. 1(b) shows the location of 18 USGS stream gauges with the corresponding contributing watershed. The terrain slope of these 18 subbasins ranges from 0.31% to 1.12% with an average of 0.64% and the area varies from 16 km^2 to 1,734 km^2 with an average of 328 km^2. In this paper, these subbasins are represented by the USGS gauge number.

Data

Rainfall data is obtained from the National Centers for Environmental Prediction (NCEP) quality-controlled Stage IV multisensor precipitation estimates (MPE) at 4 km/h spatiotemporal resolution (Du 2011). Fifteen years of data (2005–2019) is analyzed in this study with a mean annual precipitation of 912 mm for these subbasins among the study period. The streamflow observations are obtained from USGS gauges (https://waterdata.usgs.gov/nwis/rt) covering the same fifteen-year period as the precipitation data.

Due to the limited in situ soil moisture observations in the study area, model-simulated soil moisture data are utilized to provide initial conditions. The initial soil moisture content (kg/m^2) data are obtained from the North American Land Data Assimilation System Version 2 (NLDAS-v2) land surface model (LSM) at 0–40 cm depth with a spatiotemporal resolution of 12.5 km at hourly scale. Among three LSM outputs (Mosaic, Noah, and VIC LSM) from NLDAS-v2, Noah LSM is selected since it is commonly used as

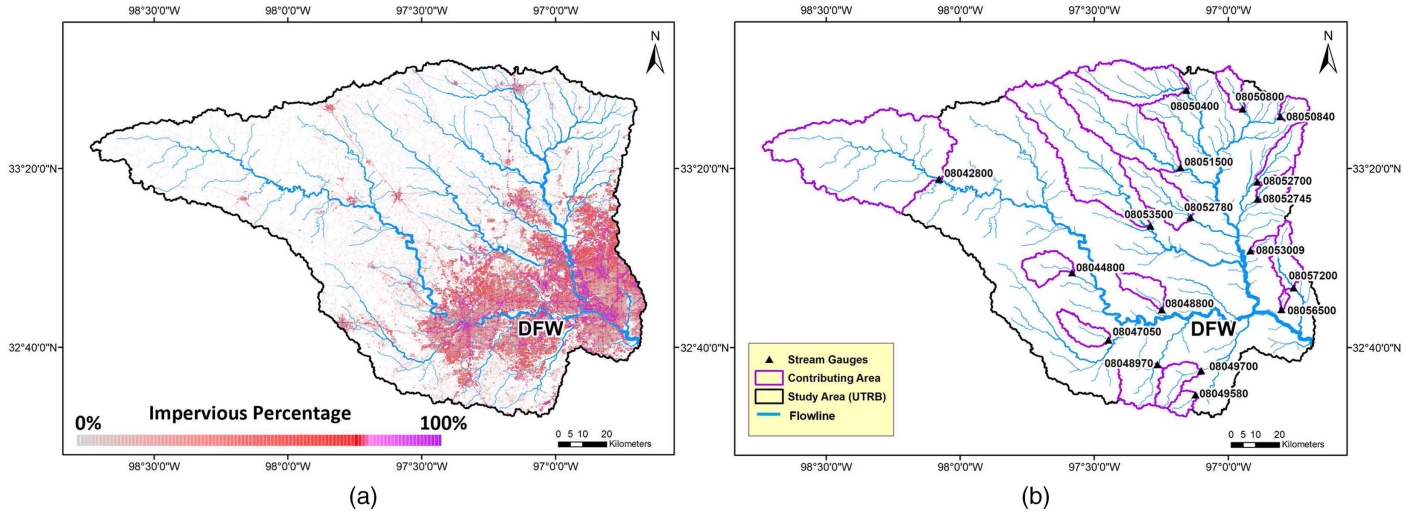

Fig. 1. Study area in the Upper Trinity River Basin (UTRB): (a) imperviousness; and (b) 18 USGS stream gauges and the corresponding contributing watershed (location data for stream gauges from USGS, n.d.).

the land surface component in multiple weather forecast systems (e.g., weather research and forecasting (WRF) regional atmospheric model, the NOAA NCEP coupled climate forecast system, and the global forecast system) (Niu et al. 2011; Yang et al. 2011). To estimate mean areal precipitation (MAP) and soil moisture at basin scale, we first resample the raw data to 1-km resolution using the nearest neighbor method, then calculate the areal average values over each subbasin. The resampling essentially increases sample size of the zonal averaging, which is especially necessary for small subbasins.

Events Selection

Runoff events are identified throughout the entire study period (2005–2019) and we use the revised constant-k method (Mei and Anagnostou 2015) to separate the baseflow from long-term hydrographs. By assuming the baseflow storage is linear, streamflow at the recession curve can be defined as in Eq. (1):

$$Q = Q_0 e^{-kt} \tag{1}$$

where Q = streamflow at time t (m^3/s); Q_0 = streamflow at the beginning of recession; and k = recession coefficient and can be rearranged as in Eq. (2)

$$k = -\frac{1}{Q}\frac{dQ}{dt} \tag{2}$$

Then the change rate of k (Δk) can be calculated as in Eq. (3)

$$\Delta k_t = \frac{k_t - k_{t-1}}{\Delta t} \tag{3}$$

As shown in Fig. 2(a), the rising limb and falling limb carry negative and positive k values, respectively. Given that k approximately reaches constant along the recession (Blume et al. 2007), the ending time of the runoff event can be identified when the change rate of k (Δk) is small enough to be considered as "no change." Fig. 2(b) illustrates the variation of Δk during a sample flow period for the watershed 08048800. Δk is stable during the recession while it shows large variation during the rising and the crest. From the variation of Δk, starting time of the event can also be identified. Then the straight-line method is applied by connecting the beginning and ending time to separate the baseflow.

Rainfall events are identified based on time series of mean areal precipitation (MAP) for each gauge/subbasin. This requires properly defining a threshold value for the minimum inter-arrival time (MIT) between any two storm events. Then we can determine whether any two positive rainfall values separated by zeros belong to the same storm event via checking whether the number of zeros is greater than MIT or not. To automate the optimization of MIT, we take the following steps as shown in Fig. 3. First, MIT is initialized at a small inter-arrival value, say 1 h. Second, a list of storm events can be identified from the MAP time series based on the initialized MIT value. Third, the inter-arrival times of the list of storm events can be calculated and fitted to an exponential distribution, which is done by assuming that storm occurrence follows Poisson process (Bove et al. 1998; Katz 2002). Fourth, the goodness-of-fit is evaluated to determine if the MIT is proper. If current MIT is not satisfactory, it will be updated by slightly increasing the value, e.g., by 1 h, and the procedure enters the next iteration starting from the first step until the updated MIT is proper. After identifying rainfall and runoff events independently, we match them by examining their overlay while minding that rainfall events should precede the runoff events.

Loss Estimation

With rainfall and runoff events identified, the total loss for each event can be calculated by subtracting surface runoff volume (i.e., the integral of hydrograph after removal of baseflow) from gross rainfall. Considering the nonlinear nature of hydrological process, a family of previous studies have discovered that surface runoff is a threshold process controlled by the antecedent wetness of the catchment (van Meerveld and McDonnell 2005; James and Roulet 2007, 2009; Latron and Gallart 2008; Penna et al. 2011). Furthermore, Detty and McGuire (2010a, b) found a clear threshold relationship between the summation of antecedent wetness and gross rainfall and runoff volume: above certain threshold, runoff volume becomes linearly correlated with the sum of antecedent soil moisture and rainfall. One of the benefits of quantifying the threshold behavior is that total loss can be easily calculated/predicted given antecedent soil moisture and gross rainfall.

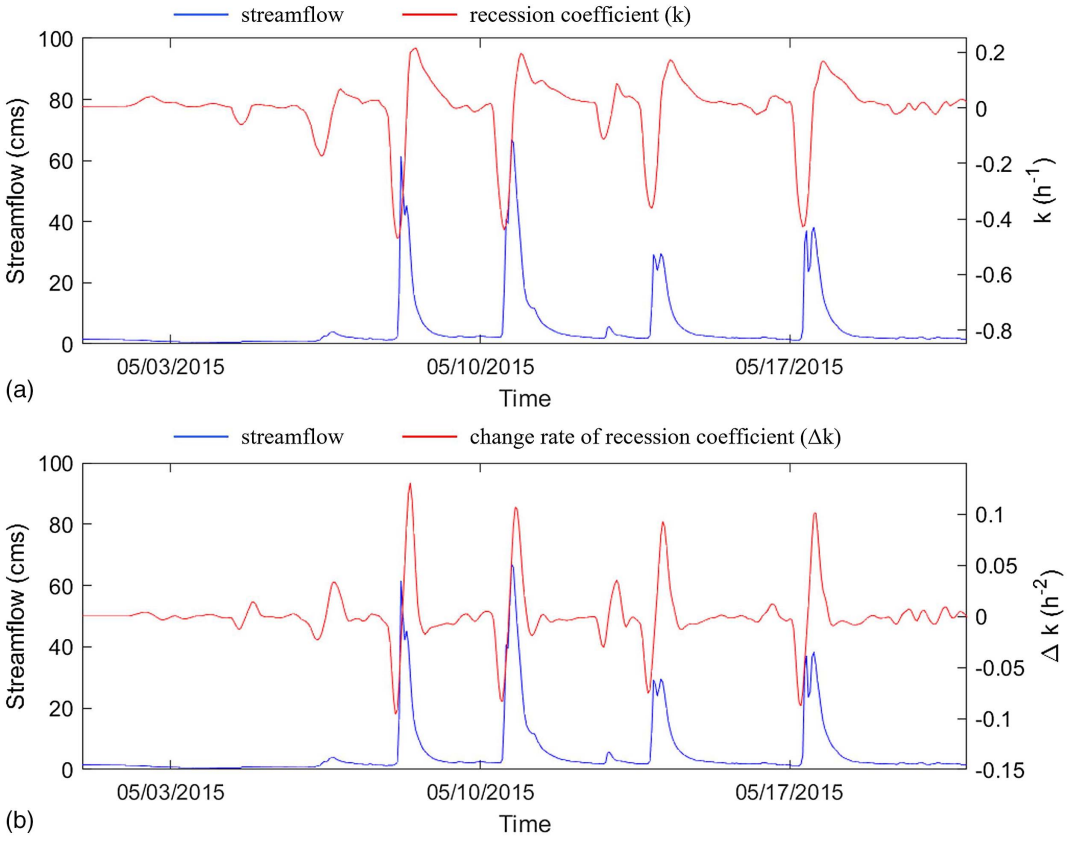

Fig. 2. Streamflow and variation of (a) recession coefficient (k); and (b) change rate of the recession coefficient (Δk) for a sample flow period of the watershed 08048800 in the Upper Trinity River Basin (UTRB).

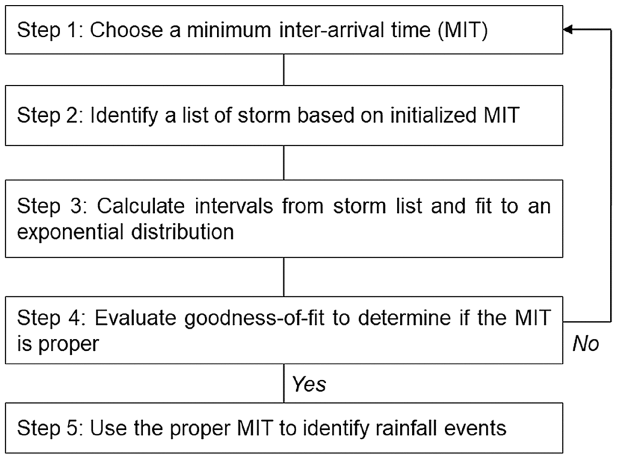

Fig. 3. Flowchart of the rainfall event identification using the minimum inter-arrival time (MIT) method.

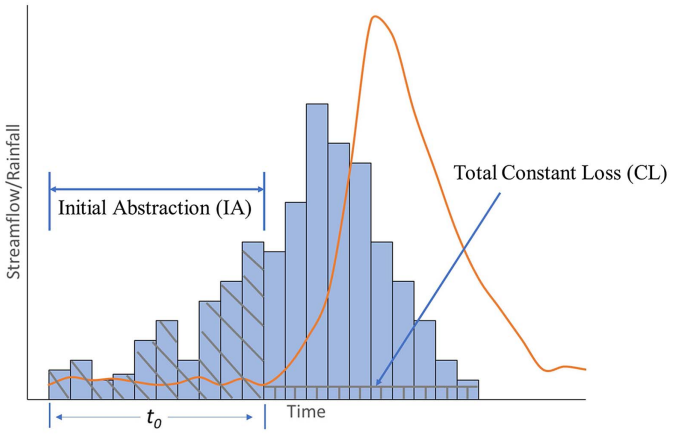

Fig. 4. Initial abstraction (IA) and constant loss (CL) for a given rainfall-runoff event.

Therefore, we evaluate this threshold behavior of the studied catchments based on observations of streamflow, rainfall and antecedent soil moisture.

When the total loss is calculated, as the components of total loss, the corresponding initial loss and constant loss can be then estimated. Based on the concept of the IACL, IA can be calculated as the amount of rainfall that occurs before the start of the runoff (Rahman et al. 2002a)

$$IA = \sum_{i=1}^{t_0} I_i \tag{4}$$

where I_i = hourly rainfall amount in mm; and t_0 = time duration (h) between rainfall starts and runoff starts as shown in Fig. 4.

The total loss volume can be expressed as:

$$\text{LOSS} = \text{Rainfall} - \text{Runoff} = \text{IA} + \text{CL} \times (t - t_0) \tag{5}$$

Table 1. Continuous probability distributions: gamma, Weibull, and lognormal distributions

Distribution	Probability density function	Parameters
Gamma	$f_X(x) = \frac{\lambda^\alpha x^{\alpha-1} e^{-\lambda x}}{\Gamma(\alpha)}$	α is the shape parameter ($\alpha > 0$) λ is the scale parameter ($\lambda > 0$) $\Gamma(\alpha)$ is the gamma function: $\Gamma(\alpha) = \int_0^\infty x^{\alpha-1} e^{-x} dx (x > 0)$
Weibull	$f_X(x) = \frac{\alpha}{\lambda}\left(\frac{x}{\lambda}\right)^{\alpha-1} e^{-\left(\frac{x}{\lambda}\right)^\alpha}$	α is the shape parameter ($\alpha > 0$) λ is the scale parameter ($\lambda > 0$)
Lognormal	$f_X(x) = \frac{1}{x}\frac{1}{\sigma\sqrt{2\pi}} e^{\left[-\frac{(\ln x-\mu)^2}{2\sigma^2}\right]}$	σ is the shape parameter μ is the location parameter

where t = rainfall duration. Note that evapotranspiration during the flood event is considered negligible, making the loss term equivalent to infiltration loss.

Then the CL can be calculated as:

$$\mathrm{CL} = \frac{\mathrm{LOSS} - \mathrm{IA}}{t - t_0} \tag{6}$$

Distribution Fitting

To analyze the probabilistic characteristics of the loss parameters, we use both parametric and non-parametric probability distributions to fit the calculated IA and CL values. Maximum likelihood estimates method is applied to fit the possible parametric distributions. Goodness-of-fit tests and plots, including the probability density function (PDF), probability-probability (P-P) and quantile-quantile (Q-Q) plots, are used to determine whether the fitted distribution is reasonable. For each fitted distribution, 10,000 random values are generated to calculate the descriptive statistics (e.g., minimum and maximum values, mean, median, standard deviation, and skewness). These statistics from fitted distributions are compared to the descriptive statistics of the sample dataset. The best fitting distribution is selected based on the results from the goodness-of-fit tests, P-P and Q-Q plots, and relative errors of the descriptive statistics. Previous studies have identified and investigated three probability distributions for IA and CL values, including gamma, Weibull and lognormal distributions (Caballero 2013; Gamage et al. 2013; Loveridge et al. 2013; Hill et al. 2016), which are therefore selected as candidates for probability distribution fitting in this study (Table 1).

In this study, Anderson-Darling test (Anderson and Darling 1952) is adopted as the goodness-of-fit test based on the empirical density function to measure how well the data fits a specified distribution. Small p-values means the data does not come from that specified distribution. When comparing with several distributions, one should choose the distribution that gives the largest p-value, which is the closet match to the data.

Results and Discussions

Rainfall-Runoff Events

Following the hydrograph separation and rainfall identification methods, we identify and pair a total of 2,036 events for 18 subbasins in UTRB. Table 2 shows the detailed number of rainfall-runoff events for each subbasin over the 15-year observation period. As shown in the rainfall and runoff statistics, a large variety of events have been covered including both small and big events.

Threshold Behavior

From the identified rainfall-runoff events for 18 subbasins in UTRB, we calculate the gross rainfall (MAP), runoff volume and total loss, and extract the antecedent soil moisture content from the top 40 cm depth of soil layer for each event. A clear threshold behavior is found for all 18 subbasins, where linear relationship of the sum of MAP and ASM gets statistically stronger beyond a threshold value (of MAP + ASM). This behavior has been reported and examined in previous studies (Detty and McGuire 2010a, b; Fu et al. 2013; Saffarpour et al. 2016). Fig. 5 shows an example (gauge 08057200) of how goodness-of-fit, indicated by the coefficient of determination R^2, changes when different threshold is selected. The R^2 is calculated based on a linear regression fit to sample points above the moving threshold. With the moving threshold increasing, the R^2 value almost increases exponentially as illustrated in Fig. 5, which means the linear relationship between MAP + ASM and runoff improves abruptly near some threshold. Therefore, one can estimate this MAP + ASM threshold accurately and conveniently by choosing some value at a high R^2.

As shown in Fig. 6, below a certain threshold, the sum of ASM and gross rainfall is poorly correlated with runoff depth, and little runoff is generated. Above this threshold value, the relationship between MAP + ASM and runoff depth becomes highly linear with R^2 values above 0.8 for most gauges in the study region (Fig. S1). The detailed statistics including the parameters of regression equations and the threshold values for each subbasin can be found in Table S2. The threshold behavior has been discovered in previous studies using small headwater catchments (area less than 10 km^2) (Detty and McGuire 2010a; Penna et al. 2011; Fu et al. 2013; Saffarpour et al. 2016). In this study, we confirm and expand the threshold behavior using more and larger-sized basins based on long-term rainfall, soil moisture, and streamflow observations. The threshold behavior can be used to estimate runoff and loss based on total rainfall and antecedent soil moisture. For example, one can predict the runoff volume for a basin using the real time soil moisture and quantitative precipitation forecast (QPF) ahead of a storm event based on the threshold behavior.

Loss Values from Selected Events

Initial and constant losses have been calculated for each event as summarized in Table 3 with the important statistics for individual gauges. The mean IA and CL values for the 18 subbasins are 27 mm and 0.6 mm/h, respectively. The average skewness values for IA and CL are 1.67 and 2.08, indicating the IA and CL distributions are positively skewed. The reason is that the lower bounds of IA and CL are zero or close to zero while the upper bounds are varied and based on the data samples. For all subbasins, the average

Table 2. Statistics of selected rainfall-runoff events for 18 subbasins

Gauge ID	Area (km^2)	Number of events	Rainfall range (mm)			Runoff range (mm)		
			Low	High	Mean	Low	High	Mean
08042800	1,733.8	15	4.87	222.88	77.60	2.42	122.65	23.34
08044800	162.5	126	0.43	145.86	38.19	0.02	59.55	5.74
08047050	142.0	265	0.11	179.23	20.85	0.07	65.22	2.46
08048800	136.5	93	0.88	121.02	31.26	0.16	44.13	7.99
08048970	233.8	152	0.19	111.92	23.48	0.08	87.09	7.13
08049580	65.9	76	1.01	106.79	34.29	0.08	96.66	11.70
08049700	163.7	203	0.10	184.26	29.79	0.05	87.41	5.45
08050400	458.9	70	0.19	517.59	51.40	0.10	349.59	17.45
08050800	101.2	37	7.36	157.20	47.48	0.16	97.83	17.61
08050840	75.9	44	4.30	145.67	34.26	1.48	92.60	14.40
08051500	758.1	57	0.43	507.67	50.91	0.10	311.74	15.53
08052700	188.9	35	1.10	179.82	47.88	1.08	165.07	24.30
08052745	98.8	80	0.80	135.30	30.41	0.16	46.00	9.23
08052780	334.3	86	1.08	179.23	37.42	0.09	109.88	9.53
08053009	35.9	177	0.46	114.50	25.45	0.16	75.37	8.84
08053500	1,033.0	29	1.73	502.06	61.52	0.35	223.32	18.39
08056500	16.3	212	0.27	116.02	23.63	0.17	73.05	7.31
08057200	172.2	279	0.71	132.38	23.20	0.14	70.87	5.87

ranges of IA and CL are 0–177 mm and 0–3.89 mm/h, respectively. Given such a wide range, using a single set of IACL values for specific design frequency, which is to convert specific rainfall (e.g., 100-year design rainfall) to streamflow (e.g., 100-year peak streamflow), seems unreliable.

To better illustrate IA and CL values with varying precipitation, we divide the data samples (2,036 events) into six groups based on 10%, 25%, 50%, 75%, and 100% percentiles of the total rainfall amount and show the ranges of IA (mm), total CL (mm) and CL (mm/h) in Figs. 7(a–c). It can be found that IA and total CL feature a small range when rainfall is little, while as rainfall gets higher, the larger variations exhibit in IA and total CL [Figs. 7(a and b)]. Here, total rainfall can be viewed as the possible maximum of IA plus total CL: as total rainfall increases, more combinations of IA and CL values are allowed, hence the larger variation. This finding is important for design applications, especially for extreme events with large rainfall amount. It may be reasonable to apply a single set of IACL for small events due to their tight ranges. However, for large events, the greater variations/ranges of IA and total CL are observed, it is questionable to assign a single set of IACL values for specific design scenario. The trend of variations in CL values is mixed as the rainfall increases [Fig. 7(c)]. This can be explained by the fact that CL is the loss rate, so it also depends on the rainfall duration other than rainfall amount.

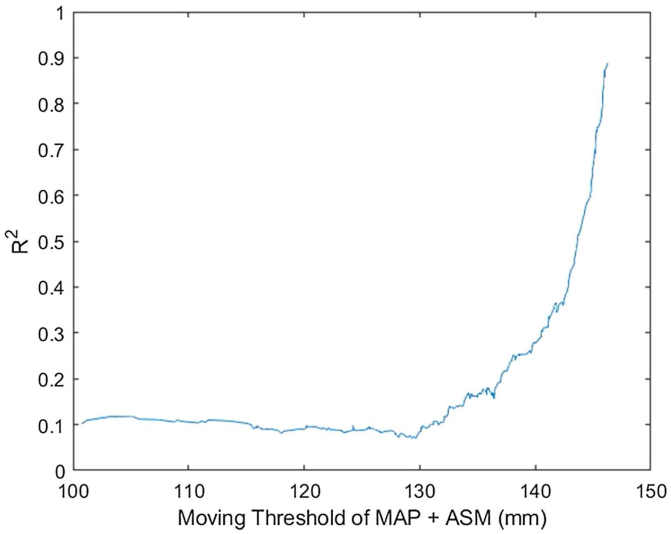

Fig. 5. Coefficient of determination R^2 calculated for a linear regression between runoff volume and MAP + ASM above a moving threshold for a sample watershed 08057200.

Distribution Fittings

Gamma, Weibull, and lognormal distributions are fitted to the calculated IA and CL values for the 18 subbasins. As shown in Table 3, identified events for some subbasins are not sufficient to generate a reasonable distribution of calculated IA and CL values. Therefore, we only show the results of distribution fittings for six subbasins which have more than 150 events identified.

Fig. 8 shows the empirical and fitted probability density functions (PDF) of gamma, Weibull, and lognormal distributions for IA values. From the goodness-of-fit statistics (Table 4), lognormal distribution is found to have the lowest p-values (less than 0.05 for most gauges), indicating poor evidence for the null hypothesis, which means lognormal is not suitable for fitting the distribution of IA. Gamma and Weibull distributions show the similar Anderson-Darling statistics. Table 5 shows the comparison of the descriptive statistics between the calculated and generated (sample size: 10,000 values) IA values from gamma and Weibull distributions. Compared with the calculated mean of IA, the gamma-generated and Weibull-generated mean both show 1% average differences from six subbasins. For the standard deviation, the average differences between calculated with gamma-generated and Weibull-generated IA are 8% and 10%, respectively. The upper limit of gamma-generated IA is closer to the calculated upper limit than Weibull. Overall, the generated IA values from gamma fitted distribution preserve statistics of the calculated IA data well.

Fig. 9 shows the empirical and fitted probability density functions (PDF) of gamma, Weibull, and lognormal distributions for CL values. From the goodness-of-fit statistics (Table 6), we can see p-values of three distributions for six gauges are all larger than 0.05, indicating the null hypothesis is not rejected. However, Anderson-Darling statistics of lognormal are always larger than

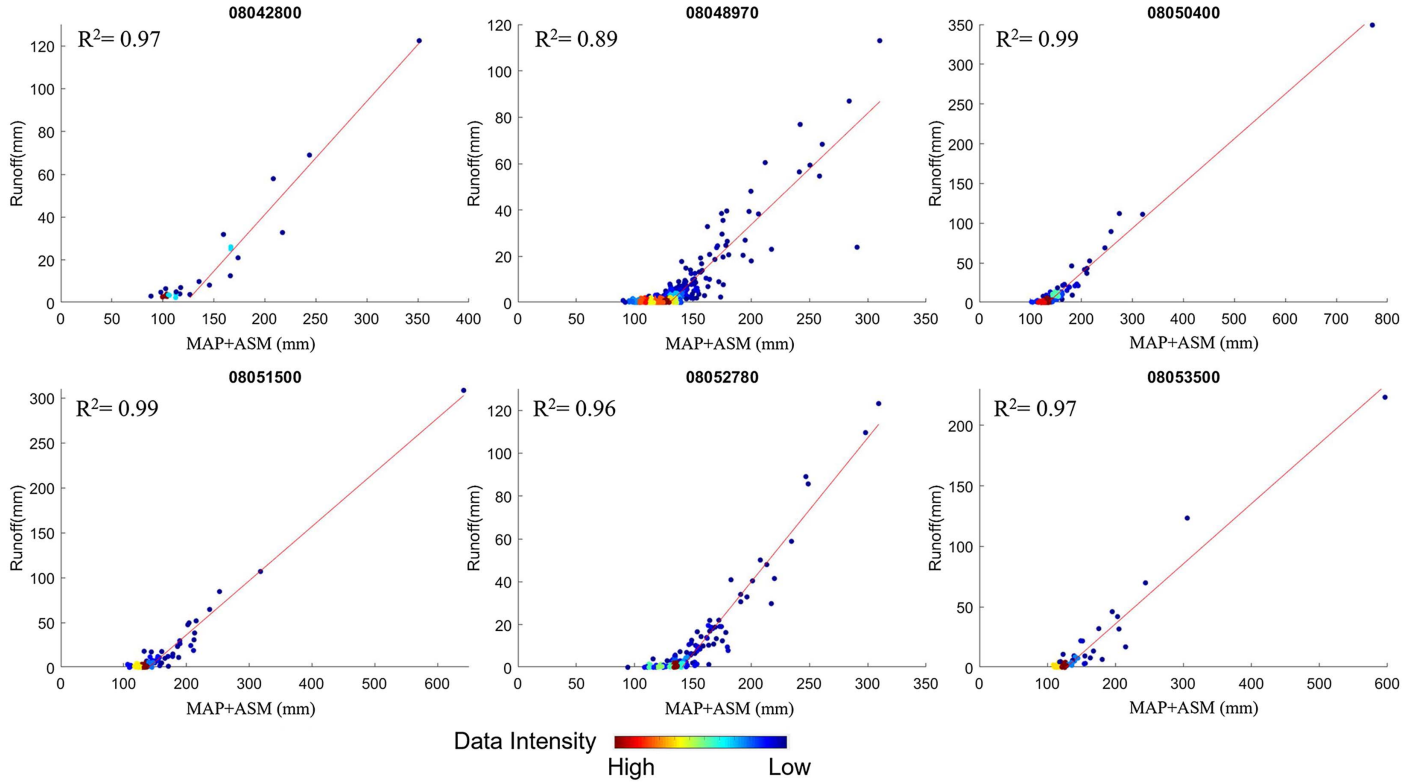

Fig. 6. Threshold behavior of the six example subbasins in UTRB.

gamma and Weibull distributions, indicating lognormal is less suitable for fitting CL compared with gamma and Weibull. Weibull has smaller Anderson-Darling statistics than gamma, meaning Weibull distribution fits CL better. Table 7 shows the comparison of the descriptive statistics between the calculated and generated (sample size: 10,000 values) CL values from gamma, Weibull, and lognormal distributions. From the statistics, we can see the fitted lognormal has much higher values for the upper limit of CL than gamma and Weibull. Compared with the calculated mean of CL, the gamma-generated and Weibull-generated mean show 1% and 2% average differences, respectively. For the standard deviation (SD), the average differences are 18% and 11% between the calculated with gamma-generated and Weibull-generated CL, respectively. The Weibull distribution is therefore found to be of best fit and well preserves statistics of the calculated CL values.

All IA and CL values from the 18 subbasins are used to extract exceedance probabilities. Figs. 10 and 11 show the resulting nonparametric distribution with 90% confidence interval for the IA

Table 3. Statistics of IA and CL values for 18 subbasins (SD meaning standard deviation)

Gauge ID	Number of events	IA (mm)					CL (mm/h)				
		Range	Mean	Median	SD	Skew	Range	Mean	Median	SD	Skew
08042800	15	5–112	49	47	33.45	0.22	0.04–0.36	0.20	0.24	0.11	−0.09
08044800	126	0–116	28	20	25.12	1.61	0.03–2.51	0.39	0.27	0.45	2.45
08047050	265	0–99	15	9	17.67	1.93	0.00–8.50	0.69	0.37	1.08	4.43
08048800	93	1–118	25	17	24.24	1.75	0.01–1.30	0.51	0.40	0.44	0.53
08048970	152	0–96	15	10	15.80	2.11	0.00–6.52	0.68	0.36	1.05	3.67
08049580	76	0–104	27	19	24.11	1.50	0.01–2.49	0.64	0.28	0.83	1.37
08049700	203	0–121	24	16	25.80	2.07	0.00–3.05	0.48	0.22	0.67	2.36
08050400	70	0–178	35	31	29.01	2.24	0.00–9.19	0.80	0.21	2.11	3.78
08050800	37	0–110	33	28	26.83	1.33	0.03–1.76	0.47	0.31	0.60	1.67
08050840	44	0–92	28	23	19.39	1.10	0.06–3.92	1.06	0.56	1.62	1.40
08051500	57	0–130	31	27	29.45	1.52	0.01–6.30	0.75	0.43	1.38	3.65
08052700	35	0–102	30	27	22.25	1.05	0.05–0.85	0.41	0.39	0.32	0.18
08052745	80	0–135	24	18	24.63	2.30	0.01–4.71	0.80	0.23	1.32	2.32
08052780	86	0–112	29	21	25.94	1.53	0.00–0.99	0.26	0.11	0.32	1.37
08053009	177	0–114	20	13	20.46	1.96	0.03–6.70	0.94	0.37	1.43	2.46
08053500	29	0–123	38	33	28.96	1.08	0.00–0.45	0.18	0.14	0.15	0.62
08056500	212	0–116	19	13	21.47	2.23	0.01–5.82	0.83	0.51	1.11	2.77
08057200	279	0–132	18	12	21.60	2.55	0.00–4.61	0.71	0.33	1.00	2.46
Average	113	0–117	27	21	24.23	1.67	0.00–3.89	0.60	0.32	0.89	2.08

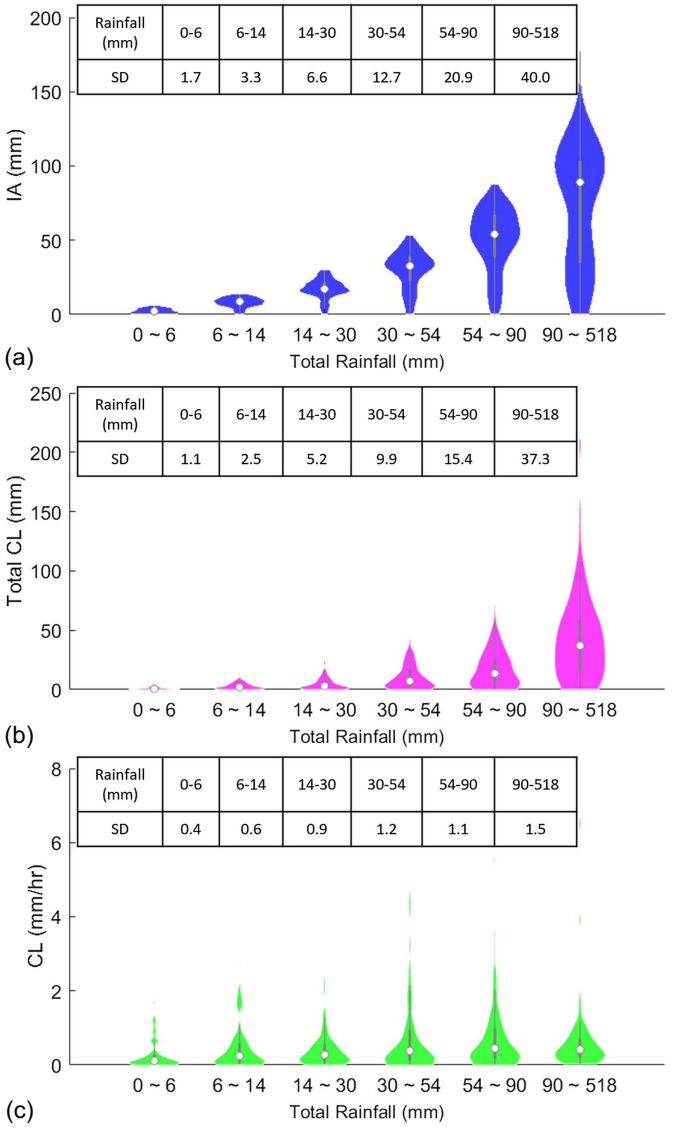

Fig. 7. Violin plots of (a) IA; (b) total CL; and (c) CL with rainfall. SD means standard deviation.

and CL values, respectively. As an alternative to the currently employed design event approach in the region (USACE 1992), random IA(CL) values for the Upper Trinity River Basin can be drawn from these statistical distributions as derived and then drive the hydrologic simulations using a Monte Carlo framework. Its main strength is that, as an event-based framework, Monte Carlo allows processes that have a dominant influence on generating and modifying floods to be represented more realistically while simplifying other less influential processes. For each model run, a set of input and parameter values (e.g., rainfall duration, rainfall intensity, rainfall temporal pattern and losses) can be randomly drawn from their respective distributions instead of choosing a default value for each variable. In particular, the drawing of random IA(CL) values can be independent by assuming no significant correlation with other inputs (e.g., rainfall) or parameters. Consequently, a Monte Carlo simulation via hydrologic modeling with the random combinations of IA and CL can generate a large sample of streamflow for deriving flood frequency curves, through which the probabilistic nature of IA and CL and other key processes are properly reflected in the design frequency flows.

Similar to the subject of this study, TxDOT and USGS also investigated IA and CL estimation in Texas using observed rainfall and runoff events. However, their derived IACL values are specifically tuned to develop gamma unit hydrographs (Asquith and Roussel 2007; Thompson et al. 2008). Using 92 applicable watersheds that cover a variety of geographic features, their study correlated some watershed characteristics (e.g., main-channel length, curve numbers) with the mean IACL values. In contrast, the 18 catchments in our study are too few to show any convincing relationships between IACL and watershed characteristics, especially when divided into multiple dimensions (multiple topographic characteristics). In other words, IA and CL values vary significantly from event to event, which overwhelms the variability across 18 catchments. Although limited by the scope of this study, we do think it would be a meaningful future effort to conduct catchment-specific probability fitting of IA and CL in a large number of catchments with a wide geographic variety and then relate distribution parameters with catchment features.

Finally, the uncertainty sources should be noted when interpreting the IA and CL estimates from this study, which is discussed in the following in the order of increasing significance. First, even though gauge-corrected Stage IV radar rainfall and USGS gauged streamflow are utilized, these quality-controlled observations are essentially estimates (with remaining errors) of the unknown truths. Second, the rainfall event separation scheme assumes that rainfall occurrence follows a Poisson process; whereas the runoff identification assumes flow recession to be controlled by a storge-discharge relationship. These statistical/empirical assumptions, though widely adopted, add uncertainties to the estimation of rainfall depth and runoff volume for storm events. Last, we consider the structural uncertainty of IACL method itself to be the greatest uncertainty source. After all, the empirical nature of IACL method deviates from the physics of infiltration process. What is more, when applied at the catchment scale, the IACL method is expected to lump the high spatial heterogeneity of the infiltration process, which could exceed how much the method can realistically approximate.

Conclusions and Future Work

This study focuses on loss estimation for the 18 headwater catchments in North Central Texas based on 15 years (2005–2019) of Stage IV rainfall and USGS streamflow data. By developing automatic retrieving schemes, we identify a total of 2,036 rainfall-runoff events and calculate the total loss with its initial abstraction (IA) and constant loss (CL) components for each event. The statistical behaviors of these IA and CL values are further explored and three distributions (gamma, Webull, and lognormal) are tested. The results of statistics and distribution fittings from this exhaustive list of events establish a solid foundation for future Monte-Carlo rainfall-runoff simulations, which promises to provide a better estimation in derived flood frequency curves. The major findings are summarized as follows:

1. Being unique from conventional approaches in identifying real storms, the automatic identification of rainfall-runoff events ensures that the occurrence of events follow a Poisson process, which can generate a large number of events that suffice the requirement in deriving statistical distribution of loss-related variables.
2. Threshold behavior is found for all studied subbasins. In UTRB, the relationship between MAP + ASM and runoff is largely linear above certain threshold values for corresponding subbasins,

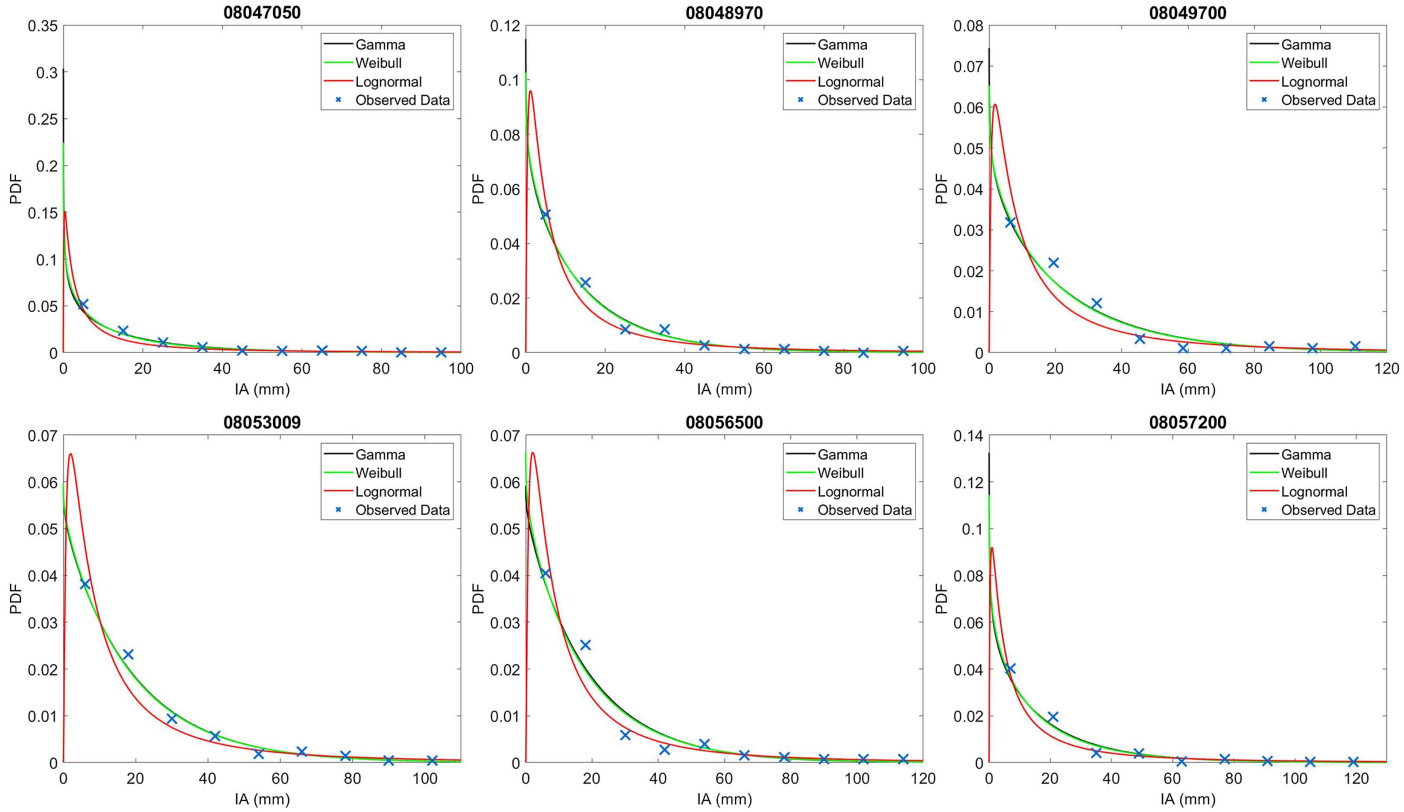

Fig. 8. Probability density functions (PDFs) of the observed data and three fitted distributions of IA values for subbasins with identified events more than 150.

Table 4. Goodness-of-fit test statistics of the fitted gamma, Weibull, and lognormal distributions of the IA data

		Anderson-Darling	
Gauge ID	Distribution	P-value	Statistics
08047050	Gamma	0.813	0.435
	Weibull	0.812	0.436
	Lognormal	0.007	4.198
08048970	Gamma	0.997	0.165
	Weibull	0.997	0.164
	Lognormal	0.093	1.991
08049700	Gamma	0.442	0.857
	Weibull	0.448	0.848
	Lognormal	0.005	4.419
08053009	Gamma	0.983	0.222
	Weibull	0.986	0.213
	Lognormal	0.068	2.236
08056500	Gamma	0.212	1.367
	Weibull	0.224	1.325
	Lognormal	0.045	2.581
08057200	Gamma	0.223	1.329
	Weibull	0.269	1.196
	Lognormal	0.001	5.650

Table 5. Comparison of statistics for the calculated and generated IA values from Gamma and Weibull distributions

	IA	Initial abstraction (IA) (mm)					
Gauge ID	number	Distribution	Range	Mean	Median	SD	Skew
08047050	265	Calculated	0–99	15.20	9.18	17.67	1.93
		Gamma	0–160	14.87	8.92	17.37	2.21
		Weibull	0–279	15.42	8.62	19.30	2.79
08048970	152	Calculated	0–96	14.76	9.74	15.80	2.11
		Gamma	0–153	14.71	9.51	15.85	2.18
		Weibull	0–151	14.59	9.53	15.61	2.24
08049700	203	Calculated	0–121	23.76	16.17	25.80	2.07
		Gamma	0–235	23.72	15.95	24.69	2.06
		Weibull	0–248	23.52	15.06	25.54	2.17
08053009	177	Calculated	0–114	19.59	13.35	20.46	1.96
		Gamma	0–197	19.36	13.21	19.65	2.14
		Weibull	0–206	19.38	13.08	19.70	2.01
08056500	212	Calculated	0–116	19.17	12.61	21.47	2.23
		Gamma	0–187	19.34	13.27	19.52	2.00
		Weibull	0–226	19.05	12.94	19.62	2.12
08057200	279	Calculated	0–132	18.06	11.95	21.60	2.55
		Gamma	0–151	17.76	11.30	19.26	2.08
		Weibull	0–223	18.05	11.40	20.37	2.40

Note: SD = standard deviation.

which indicates a convenient way to estimate/predict total loss or runoff given gross rainfall and antecedent soil moisture.

3. IA and CL can be estimated based on hyetographs and hydrographs through a simplistic framework. Estimated IA and CL can be fit to positively skewed distributions. Out of the tested distributions, Gamma is the most suitable distribution for IA while Weibull distribution has the best fit for CL.

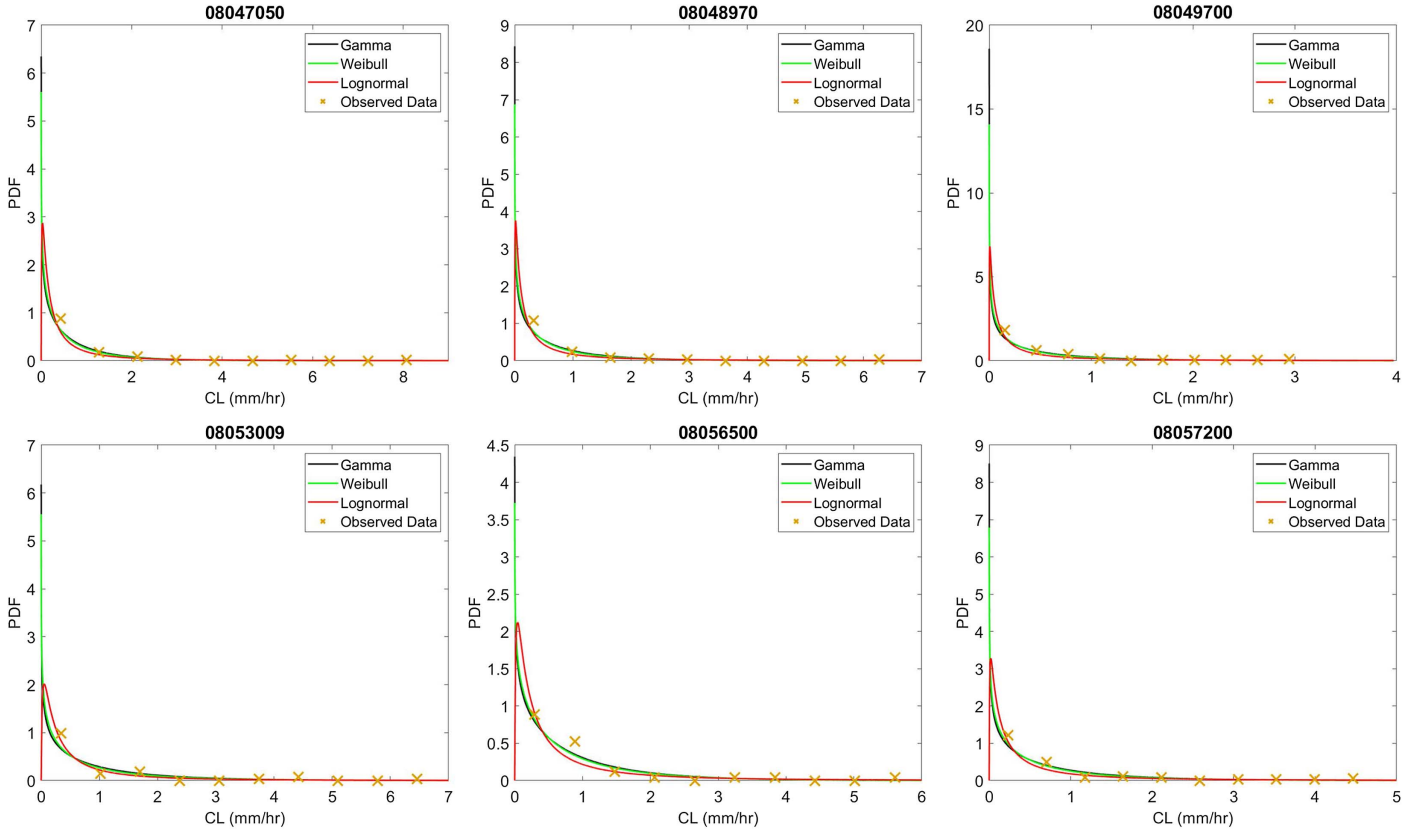

Fig. 9. Probability density functions (PDFs) of the observed data and three fitted distributions of CL values for subbasins with identified events more than 150.

Table 6. Goodness-of-fit test statistics of the fitted gamma, Weibull, and lognormal distributions of the CL data

		Anderson-Darling	
Gauge ID	Distribution	P-value	Statistics
08047050	Gamma	0.666	0.581
	Weibull	0.959	0.269
	Lognormal	0.528	0.737
08048970	Gamma	0.759	0.487
	Weibull	0.896	0.351
	Lognormal	0.355	1.004
08049700	Gamma	0.895	0.351
	Weibull	0.974	0.243
	Lognormal	0.275	1.179
08053009	Gamma	0.331	1.050
	Weibull	0.592	0.660
	Lognormal	0.277	1.236
08056500	Gamma	0.955	0.276
	Weibull	0.987	0.210
	Lognormal	0.693	0.552
08057200	Gamma	0.548	0.713
	Weibull	0.806	0.442
	Lognormal	0.340	1.034

Table 7. Comparison of statistics for the calculated and generated CL values from Gamma, Weibull, and Lognormal distributions

Gauge ID	CL number	Constant loss (CL) (mm/h)					
		Distribution	Range	Mean	Median	SD	Skew
08047050	111	Calculated	0.00–8.50	0.69	0.37	1.08	4.43
		Gamma	0.00–9.38	0.68	0.40	0.81	2.42
		Weibull	0.00–12.76	0.68	0.37	0.89	2.92
		Lognormal	0.00–94.70	0.91	0.29	2.76	15.31
08048970	52	Calculated	0.00–6.52	0.68	0.36	1.05	3.67
		Gamma	0.00–11.29	0.68	0.37	0.85	2.53
		Weibull	0.00–11.59	0.67	0.34	0.91	3.18
		Lognormal	0.00–208.72	1.10	0.27	4.11	22.17
08049700	69	Calculated	0.00–3.05	0.48	0.22	0.67	2.36
		Gamma	0.00–6.03	0.47	0.25	0.61	2.53
		Weibull	0.00–12.01	0.49	0.23	0.73	3.90
		Lognormal	0.00–558.81	0.94	0.17	6.88	60.90
08053009	40	Calculated	0.03–6.70	0.94	0.37	1.43	2.46
		Gamma	0.00–13.07	0.94	0.53	1.14	2.47
		Weibull	0.00–19.99	0.90	0.46	1.25	3.32
		Lognormal	0.00–97.48	1.00	0.37	2.44	13.96
08056500	42	Calculated	0.00–5.82	0.83	0.51	1.11	2.77
		Gamma	0.00–9.34	0.83	0.50	0.94	2.27
		Weibull	0.00–11.87	0.82	0.47	1.02	2.79
		Lognormal	0.00–86.59	1.11	0.38	2.67	10.05
08057200	77	Calculated	0.00–4.61	0.71	0.33	1.00	2.46
		Gamma	0.00–7.54	0.70	0.39	0.85	2.37
		Weibull	0.00–15.48	0.72	0.38	0.98	3.29
		Lognormal	0.00–171.24	1.06	0.29	3.66	22.53

Note: SD = standard deviation.

For future directions, we will implement the distributions of IA and CL derived from this study in a Monte Carlo framework to simulate numerous rainfall-runoff events for a flood frequency analysis. Joint distribution of loss parameters with rainfall or other

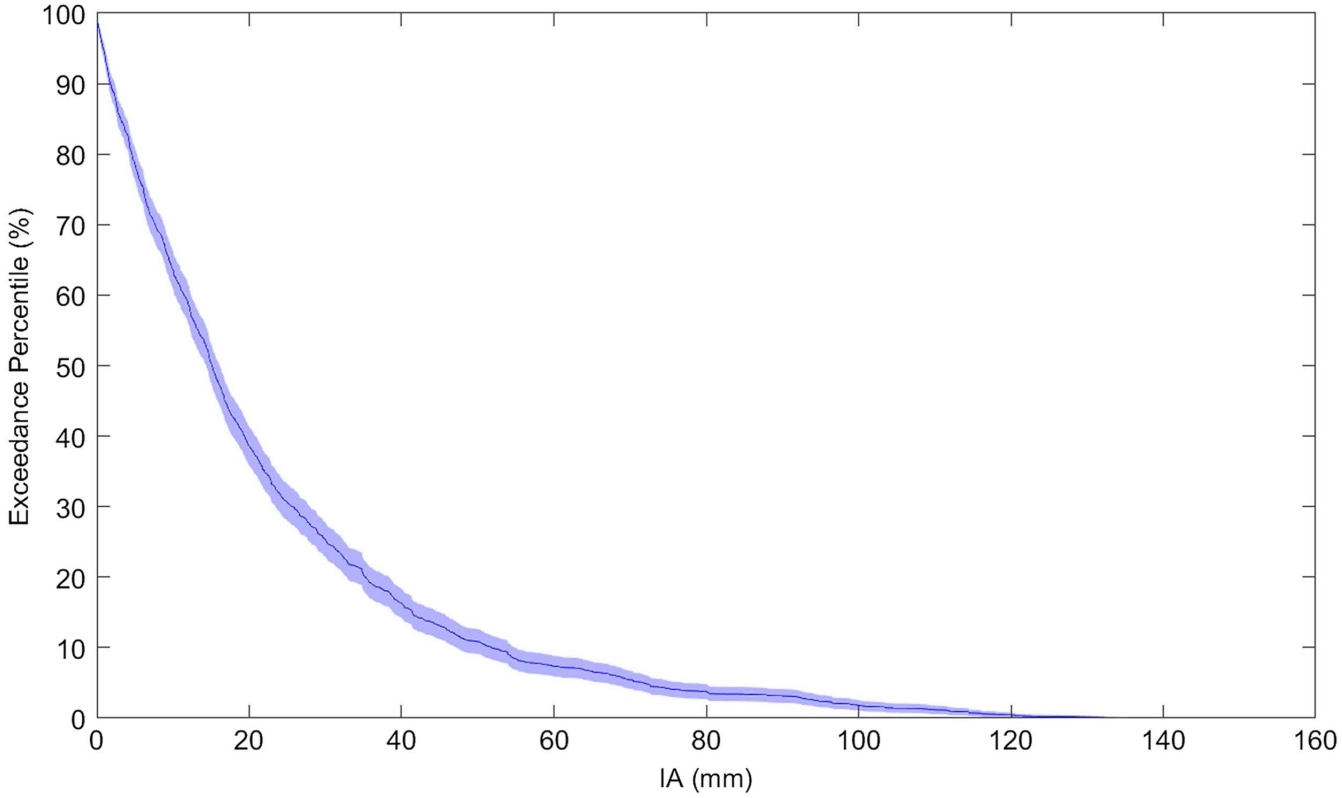

Fig. 10. Nonparametric distribution of all IA values.

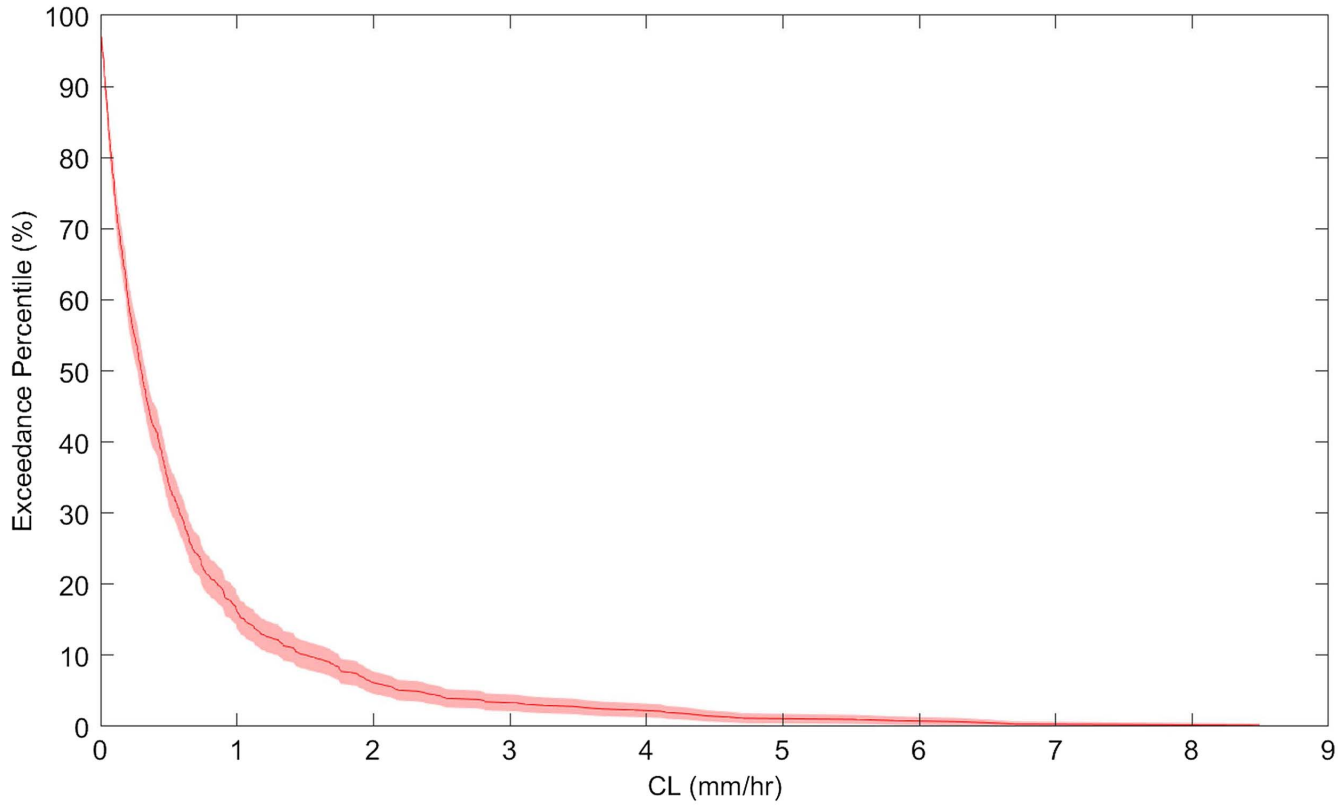

Fig. 11. Non-parametric distribution of all CL values.

influential inputs/parameters will also be considered as possible ways to capture the probabilistic nature of loss-related variables more accurately.

Data Availability Statement

Some or all data, models, or code that support the findings of this study are available from the corresponding author upon reasonable request.

Acknowledgments

We would like to thank the funding support from US Army Corps of Engineers (Project No. W9126G-17-2-SOI-0977). We also thank the three anonymous reviewers for providing insightful and constructive comments that helped us make significant improvements to the earlier version of this manuscript.

Supplemental Materials

Tables S1 and S2 and Fig. S1 are available online in the ASCE Library (www.ascelibrary.org).

References

Anderson, T. W., and D. A. Darling. 1952. "Asymptotic theory of certain 'goodness of fit' criteria based on stochastic processes." *Ann. Math. Stat.* 1952 (1): 193–212. https://doi.org/10.1214/aoms/1177729437.

Asquith, W. H., and M. C. Roussel. 2007. *An initial-abstraction, constant-loss model for unit hydrograph modeling for applicable watersheds in Texas*. Washington, DC: US Geological Survey.

Beran, M. A. 1973. "Estimation of design floods and the problem of equating the probability of rainfall and runoff." In *Proc., Symp. on the Design of Water Resources Projects with Inadequate Data, Madrid, Spain*, 33–50. Paris: UNESDOC Digital Library.

Blume, T., E. Zehe, and A. Bronstert. 2007. "Rainfall-runoff response, event-based runoff coefficients and hydrograph separation." *Hydrol. Sci. J.* 52 (5): 843–862. https://doi.org/10.1623/hysj.52.5.843.

Bove, M. C., J. B. Elsner, C. W. Landsea, X. Niu, and J. J. O'Brien. 1998. "Effect of El Niño on US landfalling hurricanes, revisited." *Bull. Am. Meteorol. Soc.* 79 (11): 2477–2482. https://doi.org/10.1175/1520-0477(1998)079<2477:EOENOO>2.0.CO;2.

Burnash, R. J. C., R. L. Ferral, and R. A. McGuire. 1973. *A generalized streamflow simulation system: Conceptual modeling for digital computers*. Sacramento, CA: Joint Federal-State River Forecast Center.

Caballero, W. L. 2013. "Enhanced joint probability approach for flood modelling." Doctoral thesis, School of Computing, Engineering and Mathematics, Univ. of Western Sydney.

Charalambous, J., A. Rahman, and D. Carroll. 2013. "Application of Monte Carlo simulation technique to design flood estimation: A case study for North Johnstone River in Queensland, Australia." *Water Resour. Manage.* 27 (11): 4099–4111. https://doi.org/10.1007/s11269-013-0398-9.

Collis-George, N. 1977. "Infiltration equations for simple soil systems." *Water Resour. Res.* 13 (2): 395–403. https://doi.org/10.1029/WR013i002p00395.

Detty, J. M., and K. J. McGuire. 2010a. "Threshold changes in storm runoff generation at a till-mantled headwater catchment." *Water Resour. Res.* 46 (Jul): 7. https://doi.org/10.1029/2009WR008102.

Detty, J. M., and K. J. McGuire. 2010b. "Topographic controls on shallow groundwater dynamics: Implications of hydrologic connectivity between hillslopes and riparian zones in a till mantled catchment." *Hydrol. Processes* 24 (16): 2222–2236. https://doi.org/10.1002/hyp.7656.

Du, J. 2011. *NCEP/EMC 4KM gridded data (GRIB) Stage IV data. Version 1.0. UCAR/NCAR*. Boulder, CO: Earth Observing Laboratory. https://doi.org/10.7158/W12-034.2013.17.1.

Eagleson, P. S. 1972. "Dynamics of flood frequency." *Water Resour. Res.* 8 (4): 878–898. https://doi.org/10.1029/WR008i004p00878.

Fu, C., J. Chen, H. Jiang, and L. Dong. 2013. "Threshold behavior in a fissured granitic catchment in southern China: 1. Analysis of field monitoring results." *Water Resour. Res.* 49 (5): 2519–2535. https://doi.org/10.1002/wrcr.20191.

Gamage, S. H. P. W., G. A. Hewa, and S. Beecham. 2013. "Probability distributions for explaining hydrological losses in South Australian catchments." *Hydrol. Earth Syst. Sci.* 17 (11): 4541–4553. https://doi.org/10.5194/hess-17-4541-2013.

Green, W. H., and G. A. Ampt. 1911. "Studies on soil physics." *J. Agric. Sci.* 4 (1): 1–24. https://doi.org/10.1017/S0021859600001441.

Heneker, T. M. 2002. "An improved engineering design flood estimation technique: Removing the need to estimate initial loss." Doctoral thesis, Dept. of Civil and Environmental Engineering, Adelaide Univ., Australia.

Hill, P., J. Zhang, and R. Nathan. 2016. *Australian rainfall and runoff revision project 6: Loss models for catchment simulation*. Canberra, Australia: Commonwealth of Australia.

Holtan, H. N. 1961. *A concept of infiltration estimates in watershed engineering*. Rep. No. ARS41-51. Washington, DC: US Department of Agricultural Service.

Horton, R. I. 1938. "The interpretation and application of runoff plot experiments with reference to soil erosion problems." *Soil Sci. Soc. Am. Proc.* 3 (6): 340–349. https://doi.org/10.2136/sssaj1939.03615995000300C0066x.

James, A. L., and N. T. Roulet. 2007. "Investigating hydrologic connectivity and its association with threshold change in runoff response in a temperate forested watershed." *Hydrol. Processes* 21 (25): 3391–3408. https://doi.org/10.1002/hyp.6554.

James, A. L., and N. T. Roulet. 2009. "Antecedent moisture conditions and catchment morphology as controls on spatial patterns of runoff generation in small forest catchments." *J. Hydrol.* 377 (3–4): 351–366. https://doi.org/10.1016/j.jhydrol.2009.08.039.

Katz, R. W. 2002. "Stochastic modeling of hurricane damage." *J. Appl. Meteorol.* 41 (7): 754–762. https://doi.org/10.1175/1520-0450(2002)041<0754:SMOHD>2.0.CO;2.

Kuczera, G., M. Lambert, T. Heneker, S. Jennings, A. Frost, and P. Coombes. 2006. "Joint probability and design storms at the crossroads." *Australas. J. Water Resour.* 10 (1): 63–79. https://doi.org/10.1080/13241583.2006.11465282.

Latron, J., and F. Gallart. 2008. "Runoff generation processes in a small Mediterranean research catchment (Vallcebre, Eastern Pyrenees)." *J. Hydrol.* 358 (3–4): 206–220. https://doi.org/10.1016/j.jhydrol.2008.06.014.

Loveridge, M., A. Rahman, P. Hill, and M. Babister. 2013. "Investigation into probabilistic losses for design flood estimation: A case study for the Orara River catchment, NSW." *Australas. J. Water Resour.* 17 (1): 13–24. https://doi.org/10.7158/W12-034.2013.17.1.

Mei, Y., and E. N. Anagnostou. 2015. "A hydrograph separation method based on information from rainfall and runoff records." *J. Hydrol.* 523 (Apr): 636–649. https://doi.org/10.1016/j.jhydrol.2015.01.083.

Mein, R. G., and C. L. Larson. 1971. *Modeling the infiltration component of the rainfall-runoff process*. Minneapolis, MN: Univ. of Minnesota.

Mein, R. G., and C. L. Larson. 1973. "Modeling infiltration during a steady rain." *Water Resour. Res.* 9 (2): 384–394. https://doi.org/10.1029/WR009i002p00384.

Mishra, S. K., J. V. Tyagi, and V. P. Singh. 2003. "Comparison of infiltration models." *Hydrol. Processes* 17 (13): 2629–2652. https://doi.org/10.1002/hyp.1257.

Mockus, V., and A. T. Hjelmfelt. 1972. *Chap 10: Estimation of direct runoff from storm rainfall*. Washington, DC: USDA, SCS National Engineering Handbook.

Niu, G. Y., et al. 2011. "The community Noah land surface model with multiparameterization options (Noah-MP): 1. Model description and evaluation with local-scale measurements." *J. Geophys. Res. Atmos.* 116 (Dec): 12. https://doi.org/10.1029/2010JD015139.

Overton, D. E. 1964. *Mathematical refinement of an infiltration equation for watershed engineering*. Rep. No. ARS 41–99. Washington, DC: US Department of Agricultural Service.

Penna, D., H. J. Tromp-van Meerveld, A. Gobbi, M. Borga, and G. Dalla Fontana. 2011. "The influence of soil moisture on threshold runoff generation processes in an alpine headwater catchment." *Hydrol. Earth Syst. Sci.* 15 (3): 689–702. https://doi.org/10.5194/hess-15-689-2011.

Philip, J. R. 1957. "The theory of infiltration." *Soil Sci.* 84 (3): 257–264. https://doi.org/10.1097/00010694-195709000-00010.

Philip, J. R. 1969. "Theory of infiltration." In *Advances in hydroscience*, edited by V. T. Chow, 215–296. New York: Academic Press.

Pilgrim, D. H., and I. Cordery. 1975. "Rainfall temporal patterns for design floods." *J. Hydraul. Div.* 101 (1): 81–95. https://doi.org/10.1061/JYCEAJ.0004197.

Rahman, A., E. Weinmann, and R. G. Mein. 2002a. "The use of probability-distributed initial losses in design flood estimation." *Australas. J. Water Resour.* 6 (1): 17–29. https://doi.org/10.1080/13241583.2002.11465207.

Rahman, A., P. E. Weinmann, T. M. T. Hoang, and E. M. Laurenson. 2002b. "Monte Carlo simulation of flood frequency curves from rainfall." *J. Hydrol.* 256 (3–4): 196–210. https://doi.org/10.1016/S0022-1694(01)00533-9.

Richards, L. A. 1931. "Capillary conduction of liquids through porous mediums." *Physics* 1 (5): 318–333. https://doi.org/10.1063/1.1745010.

Saffarpour, S., A. W. Western, R. Adams, and J. J. McDonnell. 2016. "Multiple runoff processes and multiple thresholds control agricultural runoff generation." *Hydrol. Earth Syst. Sci.* 20 (11): 4525–4545. https://doi.org/10.5194/hess-20-4525-2016.

Singh, V. P., and F. X. Yu. 1990. "Derivation of infiltration equation using systems approach." *J. Irrig. Drain. Eng.* 116 (6): 837–858. https://doi.org/10.1061/(ASCE)0733-9437(1990)116:6(837).

Smith, R. E. 1972. "The infiltration envelope: Results from a theoretical infiltrometer." *J. Hydrol.* 17 (1–2): 1–22. https://doi.org/10.1016/0022-1694(72)90063-7.

Thompson, D. B., T. G. Cleveland, D. B. Copula, and X. Fang. 2008. "Lost-rate functions for selected Texas watershed." Accessed June 1, 2020. http://www.techmrt.ttu.edu/reports.php.

USACE. 1992. *Upper trinity river reconnaissance study.* Washington, DC: USACE.

USACE. 2013. *Corridor development certificate (CDC) –Upper Trinity River, Texas –Hydrologic and hydraulic model update*. Washington, DC: USACE.

USGS. n.d. "National water information system." Accessed March 1, 2020. https://waterdata.usgs.gov/nwis/rt.

van Meerveld, I. T., and J. J. McDonnell. 2005. "Comment to "Spatial correlation of soil moisture in small catchments and its relationship to dominant spatial hydrological processes." *J. Hydrol.* 303 (1–4): 307–312. https://doi.org/10.1016/j.jhydrol.2004.09.002.

Viglione, A., R. Merz, and G. Blöschl. 2009. "On the role of the runoff coefficient in the mapping of rainfall to flood return periods." *Hydrol. Earth Syst. Sci.* 13 (5): 577–593. https://doi.org/10.5194/hess-13-577-2009.

Yang, Z. L., et al. 2011. "The community Noah land surface model with multiparameterization options (Noah-MP): 2. Evaluation over global river basins." *J. Geophys. Res.: Atmos.* 116 (Dec): 12. https://doi.org/10.1029/2010JD015140.